EGTRIB Journal
JOURNAL OF
THE EGYPTIAN SOCIETY OF TRIBOLOGY
VOLUME 20, No. 4, October 2023, pp. 12 – 26 **ISSN 2090 - 5882**
(Received June 28. 2023, Accepted in final form August 18. 2023) **jest.journals.ekb.eg**

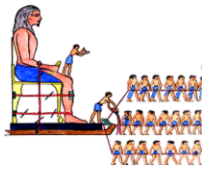

INFLUENCE OF MULTI-PASS GTAW PARAMETERS ON MICROSTRUCTURE CHARACTERIZATION AND MECHANICAL PROPERTIES OF SAF 2507 SUPER DUPLEX STAINLESS STEEL

Ali A. S.[1], Mohamed M. El-Sayed Seleman[2], Mohamed M. Z. Ahmed[2, 3], Elsoeudy R . I.[1], Eslam Abd Elaal Mahmoud[4] and Madeha Kamel[1]

[1]Mechanical Engineering Dept., Faculty of Engineering, Suez Canal University, EGYPT,
[2] Department of Metallurgical and Materials Engineering, Faculty of Petroleum and Mining Engineering, Suez University, Suez 43512, Egypt,
[3] Mechanical Engineering Dep., College of Engineering at Al Kharj, Prince Sattam Bin Abdulaziz University, Al Kharj 16273, Saudi Arabia,
[4] Siemens-energy Company, Cairo, Egypt.

ABSTRACT
In the present work, a 6 mm thickness SAF 2507-SDSS were welded by multi-pass gas tungsten arc welding (GTAW) process with ER2594 electrode using different heat inputs. Microstructure and mechanical properties of SAF 2507 joints obtained from multi-pass GTAW processes were investigated. The obtained joint was evaluated and characterized by using visual inspection, radiographic test, liquid penetrant test, optical microscopy, scanning electron microscopy, tensile and hardness test. The results obtained have shown that the type of filler electrode, heat input, and interpass temperature are the controlling factors in achieving a sound weld joint. The multi-pass GTAW of 2507 SDSS exhibited an enhancement in both hardness and yield strength compared to the base metal. In the welded zone, there were three distinct forms of austenite: Widmanstatten austenite (WA), intra-granular austenite (IGA), and grain boundary austenite (GBA), along with the presence of ferrite. The number of welding passes and heat input had a significant impact on the α:γ ratio. The content of ferrite in the welded zone is relatively close to the equilibrium ratio of the base metal and did not exhibit significant fluctuations when employing various welding parameters.

KEYWORDS
GTAW, mechanical properties, SAF 2507 SDSS, ferrite content, heat input, microstructure.

INTRODUCTION
The microstructure of duplex stainless steel (DSS) comprises an equal amount of ferrite and austenite, [1 - 3], affording it the advantages associated with both phases.

Super duplex stainless steels (SDSSs), an advanced iteration of DSS, feature an increased chromium (Cr) content, resulting in even greater corrosion resistance compared to DSS, [4, 5]. Recognizing the significant role of nitrogen as an alloying element represents a substantial advancement in enhancing the weldability, tensile strength, and corrosion resistance of DSS and SDSS. In the solidification process of DSS and SDSS, the microstructure is initially entirely ferritic; subsequently, the transformation from ferrite to austenite begins, [6, 7].
Today, these alloys find extensive use in industrial sectors such as oil and gas, Mining, marine, as well as in petrochemical industries, [8 - 11]. Duplex stainless steels (DSSs) typically exhibit commendable resistance against stress corrosion cracking, pitting, and general corrosion. They also possess high tensile strength, fatigue resistance, and reasonable weldability. To ensure that DSS and SDSS joints attain the desired properties, it is imperative to maintain a balanced 50/50 proportion of austenite and ferrite within the microstructure post-welding. Furthermore, the absence of any undesirable phases, like Cr_2N, holds significant importance in this regard, [12].

The pitting corrosion resistance of these alloys relies on their chemical composition. To gauge their resistance to pitting corrosion, a parameter called the pitting resistance equivalent number (PREN) is employed. This metric also aids in comparing the pitting resistance across various grades. Under this criterion, DSSs possessing PREN values equal to or greater than 40 are categorized as SDSS, [6, 7]. Past studies have demonstrated that the most desirable weld properties are achieved when there is an even 50/50 phase balance within the microstructure, [13].

welding is an indispensable joining method. Gas tungsten arc welding (GTAW) stands out as one of the most widely employed methods for joining these alloys. Various parameters are affecting weldment properties during the welding process, exerting an influence on the properties of the resulting weldments. Among these factors, heat input assumes a critical role in controlling the balance between ferrite and austenite phases, [12, 14].

Many researchers have investigated the impact of heat input on weld properties, [15 - 17]. A gradual cooling process promotes the formation of an adequate amount of austenite, thereby attaining a 50/50 phase equilibrium. Nevertheless, a slow cooling rate within the precipitation range may lead to the formation of undesirable intermetallic phases within the ultimate microstructure, [18]. It is important to note that elevated heat input can lead to a rise in the maximum temperature. However, it is important to remember that the primary solidification phase in SDSS is ferrite.

According to the significant influence of heat input on weldment characteristics, researchers have suggested specific heat input ranges that can yield the desired properties. For DSSs, this range falls between 0.5 and 2 kJ/mm^2, while for SDSS, it extends from 0.2 to 2 kJ/mm^2, [17, 19 - 21].

However, when it comes to GTAW welding of stainless steel, it is crucial to give thoughtful attention to various parameters, including the choice of electrode, configuration of current and voltage settings, control of travel speed, and considerations for preheat and post-weld heat treatment, [22 - 24]. Selecting the right electrode, typically one made of duplex stainless steel, ensures a harmonious match

in composition and mechanical properties between the filler material and the base metal. Achieving an equilibrium in heat input necessitates making appropriate adjustments to current, voltage, and travel speed.

In this respect, Paulraj and Garg, [4], conducted an evaluation of how various welding parameters influence the corrosion characteristics of joints in both DSS and SDSS. Among the parameters examined, heat input was a significant focus. Elevated levels of heat input resulted in the formation of larger grains and a higher proportion of austenite. Furthermore, an increase in heat input correlated with elevated corrosion rates, attributed to the development of intermetallic phases at these higher heat input levels, which compromised corrosion resistance. Their conclusion was that lower heat input values yielded joints with superior resistance to corrosion.

The objective of this study is to assess how multiple passes of Gas Tungsten Arc Welding (GTAW) parameters influence the welding process of 6 mm thick plates of 2507-SDSS. Additionally, the impact of multi pass GTAW on the microstructure and mechanical properties of the weldment.

EXPERIMENTAL WORK

Material

SAF 2507-SDSS plates with a thickness of 6 mm, dimensions of 200 mm in length and 100 mm in width, were employed as the starting materials. These plates, sourced from RAHUL Company located in Bogra, Bangladesh, had their chemical composition detailed in Table 1, as provided by the supplier.

Table 1 Chemical combination of the 2507-SDSS.

Element	Cr	Ni	Mo	Mn	Si	P	C	S	Fe
(wt. %)	26	8	5	1.2	0.8	0.035	0.03	0.02	Bal.

Gtaw procedure of 2507-sdss

The GTAW method was employed for the entire welding process, including root, filling, and final passes, using a 2.4 mm diameter ER2594 filler metal rod. The GTAW welding procedure for the 2507-SDSS followed the guidelines outlined in ASME code section IX and was performed using the Magmaweld RS 500 M manual GTAW machine, Istanbul, Turkey. To avoid detrimental effects associated with excessive heating on the properties of the welded SDSS alloys, [8], preheating was not applied. Furthermore, the maximum temperature during the GTAW inter-pass did not exceed 100 °C, as recommended to minimize the formation of intermetallic phases. Table 2 provides the composition of the ER2594 welding consumable rod. Compared to the 2507-SDSS, the ER2594 filler rod contains 2.2% more nickel to facilitate the transformation of solid delta α into γ, [13]. Figure 1 illustrates a schematic drawing of the butt weld joint design for the 2507-SDSS, featuring a 60◦ V-shape groove with a 2 mm root face and a 4 mm root gap. Detailed information

regarding the GTAW process for the 2507-SDSS is presented in Table 3. A manual stainless steel brush was used to remove oxide scales during the GTAW process.

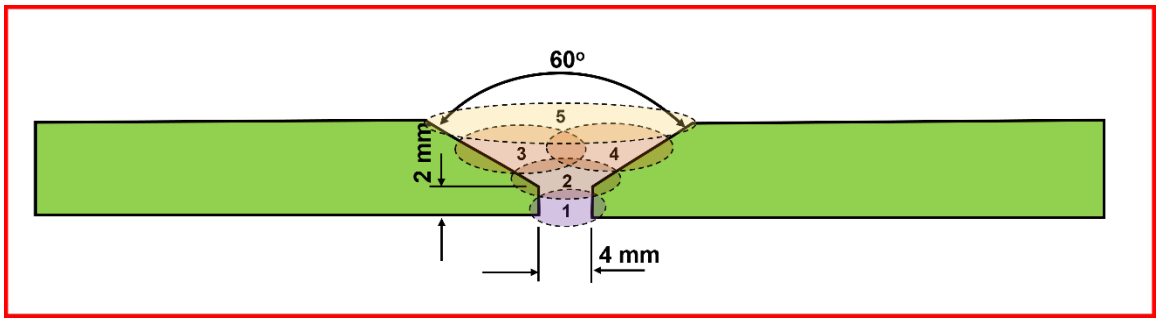

Fig. 1 Joint configuration of the 2507-SDSS for the GTAW process.

Table 2 The chemical composition of the ER2594 (in wt. %).

Element	Cr	Ni	Mo	Mn	Si	C	P	S	Fe
Content (wt. %).	27.2	8.69	2.88	1.59	0.9	0.043	0.012	0.013	Bal.

Table 3 GTAW welding parameter.

Pass No.	Interpass temp. °C	Electrode	Amps	Volt	Travel speed mm/min	Heat input J/mm
1	-	ER2594 – 2.4 mm diameter	94	10.2	45	1278
2	70		105	10.6	70	954
3	87		110	11.5	90	843
4	100		120	12.2	95	947
5	92		105	12	90	840

Characterization of welded joints

Following the GTAW process, a series of non-destructive tests were employed to assess the welded joint for any potential defects, both on the surface and within the internal regions. These tests included visual inspection, liquid penetrant testing, and radiographic testing. Visual inspection provided real-time evaluation of the surface condition, allowing for the detection of visible defects like large cracks, corrosion, surface irregularities, or improper welds. This immediate assessment allowed for prompt corrective actions to be taken. The liquid penetrant test, also known as the

dye penetrant test, was employed to identify surface defects such as cracks, surface porosity, and material discontinuities in the welded joint. For examining the internal structure of the materials and identifying any defects or discontinuities, a radiographic test (RT) was conducted. This test used a Gamma-ray camera (Model 880 MAN-027, NSW, Australia) with a Gamma ray source (Iridium-192) and AGFA D7 radiographic films. Following the completion of these non-destructive tests, the welded joint was sectioned perpendicular to the welding direction using a wire cut machine (Model JOEMARS AWT655S, Taichung, Taiwan). The sections were then subjected to microstructure analysis, macrostructure evaluation, hardness testing, and tensile testing. To analyze the microstructure, the polished cross-section of the joint was treated with a CuCl2 solution in HCl and ethanol. Optical microstructure analysis was carried out using a microscope (Model Olympus BX41M-LED, Tokyo, Japan), while field emission scanning electron microscopy (SEM) was employed for detailed analysis (Model Zeiss EVO10, Carl Zeiss AG, Oberkochen, Germany). Phase analysis in the weld zone was performed to determine the presence of α and γ phases using a ferrite scope (Model Fischer FMP30, Worcestershire, UK). Vickers hardness testing was conducted on the cross-section of the welded joint using a Vickers Hardness Tester machine (HWDV-75, TTS Unlimited, Osaka, Japan) with a 2000 gf load and a dwell time of 15 seconds. Tensile specimens were extracted in a direction perpendicular to the welding direction, prepared in accordance with ASTM E8/E8M-16a [25], with the dimensions outlined in Figure 2. The tensile test was carried out at room temperature using a universal test machine (Instron 4208, 300 kN capacity, Norwood, MA, USA) with a ram head-speed of 0.5 mm/min.

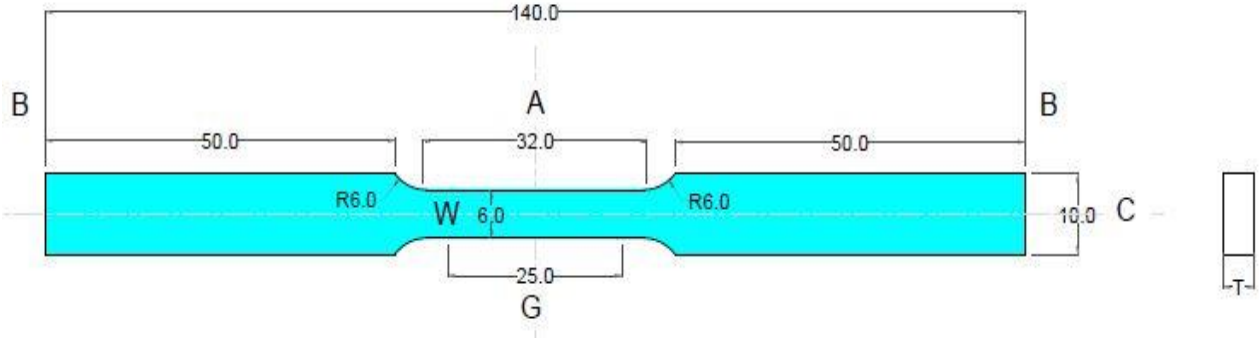

Fig. 2 Dimensions of the tensile test specimen according to ASTM E8 (dimensions in mm).

RESULTS AND DISCUSSION

Nondestructive test results

The top view of SAF 2507 SDSS with multi pass GTAWed shows in figure 3a. Through visual inspection. The obtained joint using the design V- groove shape with an angle of 60^0, a root face of 2 mm, and a root gap of 4 mm, no defects are detected indicating excellent surface appearance of multi pass GTAW. Figure 3 (b, c) shows the liquid penetration test and radiography images, respectively of the welding joint after GTAW. For liquid penetration test it was observed that, a very favorable surface appearance was observed, reflecting good surface conditions devoid of any discernible defects. on the other hand, radiography image revealed that no internal

defects detected along the joint length, that is due to suitable joint design, suitable welding parameters, and adequate material flow.

Fig. 3 (a)Top view of 2507 SDSS with multi pass GTAW, (b) image for liquid penetration test of 2507 SDSS with multi pass GTAW, (c) Radiographic images of the 2507 with multi pass GTAW.

Microstructure and macrostructure evaluation

The macrostructure image of the transverse cross-section of the GTAWed joint presents in Fig. 4 a. By employing a V-shaped groove with a 2 mm root face and a 4 mm root gap, a sound joint was obtained by using multi pass GTAW. Figure 4b shows the optical microstructure of the BM for 2507 SDSS where both ferrite (α) and austenite (γ) are easily identified. Moreover, the fusion welding characteristics of the welded joint reveal the presence of two distinct zones, the weld zone (WZ) and the heat-affected zone (HAZ)[26].Some microstructural changes take place in the WZ region resulting in inter-granular austenite (IGA), grains boundaries austinite (GBA) and Widmanstätten austenite (WA), as shown in figure 4c. The different welding zones with different magnifications are presentss in figure 4 (d, e).

It is important to note that achieving the desired microstructure in the weld zone is crucial for maintaining the mechanical and corrosion-resistant properties of the 2507 SDSS. Careful control of welding parameters, including heat input and cooling rate, is necessary to optimize the microstructural features and ensure the integrity of the welded joint. During the GTAW process, the high temperatures reached during welding cause the austenite to transform into a coarser grain structure. This can lead to the formation of Widmanstätten austenite (WA), which appears as elongated or lath-like structures. the microstructure of HAZ comprises large grains of α-phase with interconnected γ phase networks on the α grains boundaries (GBA) and smaller grains of Widmanstatten austenite (WA). Additionally, there is presence of intra-granular and grain boundary austenite (IGA), which form within the ferrite grains.

Widmanstatten austenite (WA), intra-granular austenite (IGA) and grain boundaries austenite (GBA) are significant features of the microstructure for all heat inputs [1,26,27]. for the current investigations, no intermetallic are observed in the weld zone across all the applied heat inputs.

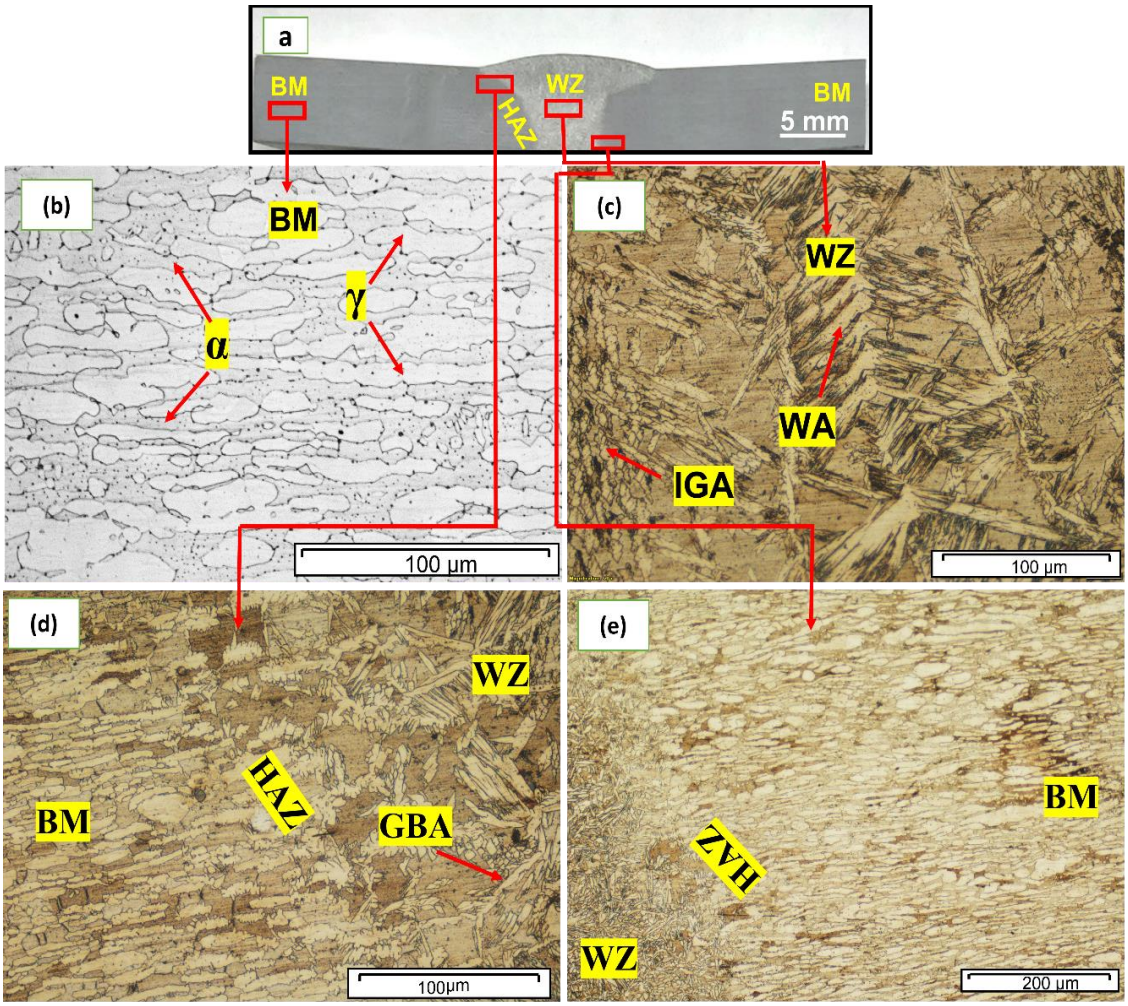

Fig. 4 (a) Macrostructure image of 2507 SDSS with multi pass GTAWed joint, (b) Opticalmicrostructure image of the BM, (c) Optical microstructure image of WZ, (d, e) Optical Microstructural images of the various zones. for GTAWed joint.

Ferrite content measurement

Figure 5 shows the percentage of α content during measurement by using a ferrite-scope type FERITSCOPE MP30 for the weld joint of 2507 SDSS produced through the multi pass GTAW technique. The ferrite content measurement results of the welded joint of 2507 SDSS employing multi-pass GTAW are summarized in Table 4. The measurements reveal that in the base metal (BM), the α and γ percentage phases are 50.6% and 49.4%, respectively. These findings align closely with previous reports by other authors on the as-received 2507 SDSS, [5, 26, 28]. Furthermore, α: γ phase ratio for the GTAWed joint is determined to be 43: 57. These phase ratios are relatively close to the balance ratio of α and γ in the BM. According to previous

studies, the welded joint can be classified as a high-quality joint when the γ phase percentage in the DSS welded joint surpasses 30 %, [27]. The weld zone of the GTAWed joint exhibits a higher austenite proportion (57 %) compared to the BM (47 %). This increase can be attributed to the utilization of ER2594 wire during the welding process, which contains a higher nickel content than the 2507 SDDS. Meanwhile, the multi pass GTAW technique which applied in this study maintained the α and γ phases without inducing ferritization. Therefore, these results endorse the use of multi pass GTAW for welding 2507 SDSS, specifically under the recommended welding conditions established in the current work, while preserving the desired α:γ ratio.

Fig. 5 Ferrite percentage content during measurement by using a ferrite-scope.

Table 4 ferrite content measurements for 2507 SDSS BM, WZ of the GTAWed joint.

Samples	Readings of ferrite No. (%)					AV. Reading of α phase	Calculated γ Phase
BM	52	49	50	51	51	50.6	49.4
GTAW	44	44.3	40	44.7	42	43	57

Hardness and tensile characteristics

The hardness profile of the 2507 SDSS produced through the multi pass GTAWed presents in figure 6. Hardness measurements were conducted along two transverse lines spanning the cross-section of the welded joints. It is evident that the maximum hardness values reach up to 348 HV at the center of the stir zone. The hardness gradually decreases as we move to the HAZ, with value of 269 HV. compared to the as-received base material (BM), the hardness value is 310 HV. The variations in hardness within the weld zone can be attributed to differences in the microstructure, particularly in terms of the morphology and distribution of micro-constituents, [26]. The presence of an increased amount of γ phase enhances the hardness of the WZ, [29, 30] . Conversely, the presence of significantly coarser ferrite grains in HAZ leads to a decrease in hardness.

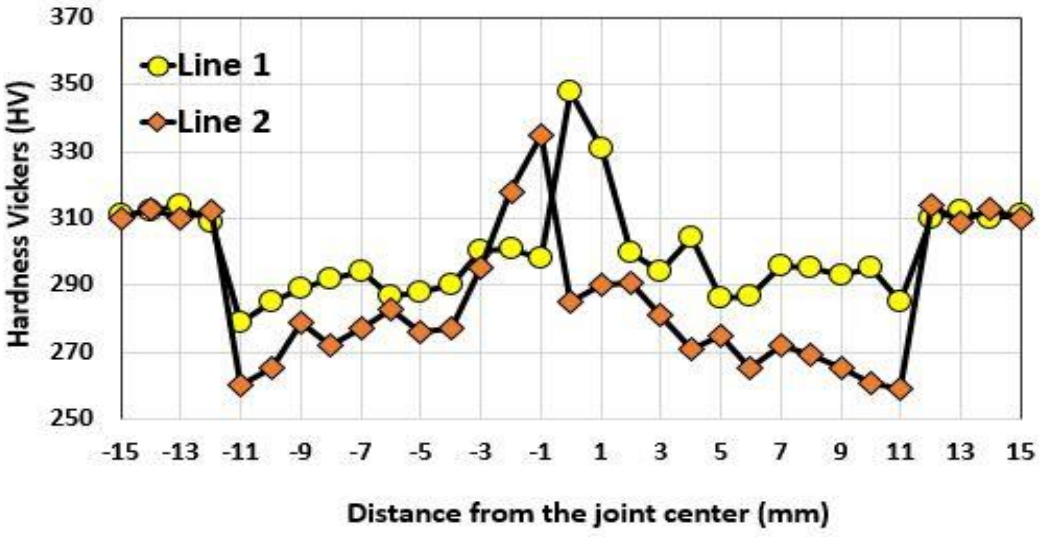

Fig. 6 Vickers hardness profile of the 2507 SDSS of GTAW joint.

Figure 7 (a, b) shows the tensile test specimen of the BM and welded joint before the test. During, after conducting the test, figure 8a presents the sample during the tensile test, figure 8b displays the fracture location occurred at the HAZ indicated in the red circle. Tensile properties including ultimate tensile stress (UTS), yield stress (YS), and elongation (E%) for the GTAWed joint, compared to the BM are shows in figure 9. it is clearly observed that the UTS value for BM sample of 1273 MPa is relatively close to the GTAWed sample value of 1163 MPa. the E% values for BM sample is 50 % which is larger than the GTAWed sample of 30 %. When looking at the YS values, it can be observed that GTAWed sample obtain the highest value compared to the BM sample, which the YS value for GTAWed joint is 801 MPa, the YS value for BM is 503 MPa. A noticeable enhancement of approximately 59% in the yield strength detected for the GTAWed joint over the Ys of the BM. The observed increase in yield stress may be attributed to the grain refinement in the WZ, [31].

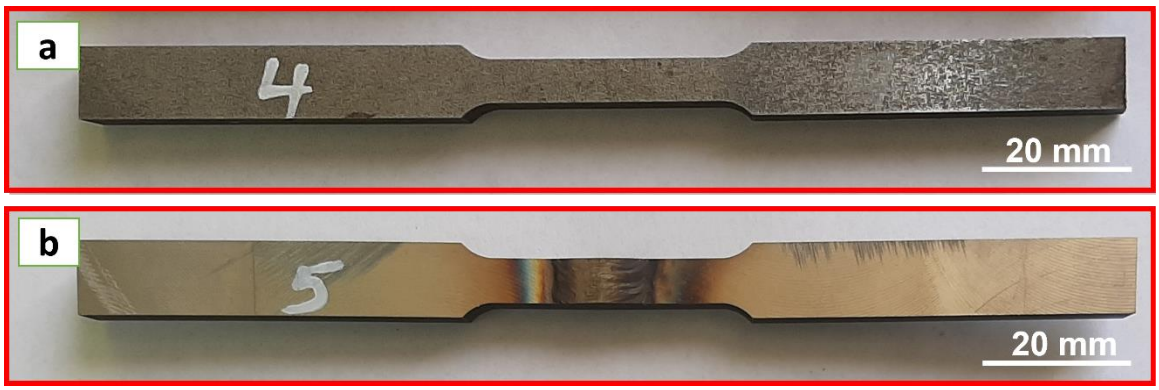

Fig. 7 Tensile test specimen of (a) the BM, (b) The GTAWed joint before tensile test

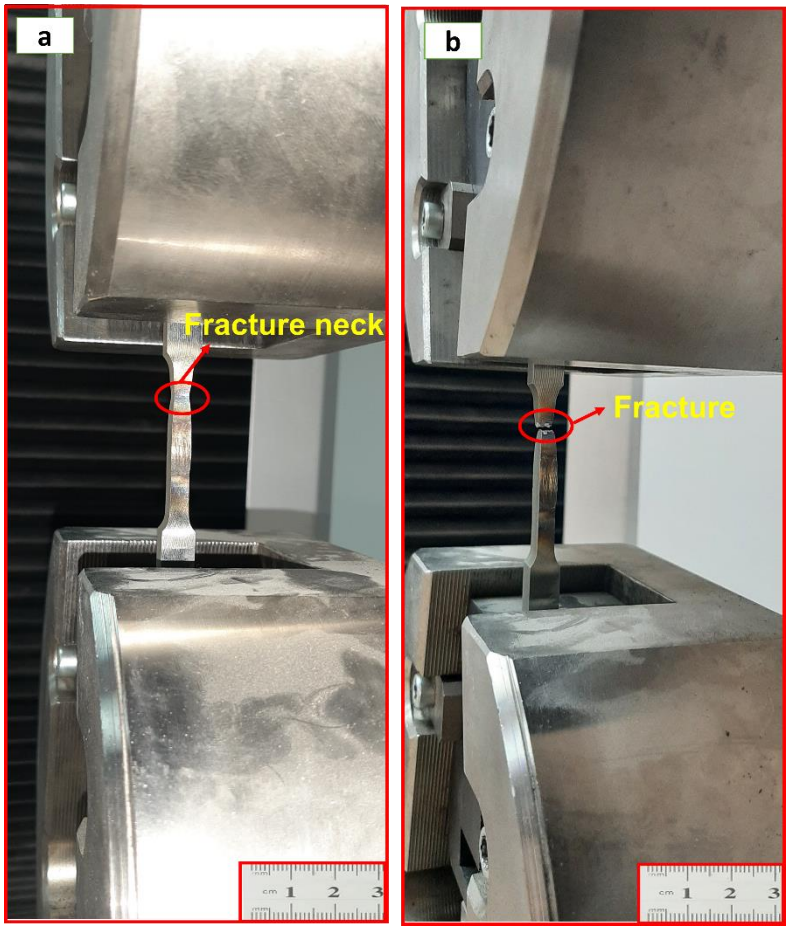

Fig. 8 (a) The specimen of welded joint during the tensile test, (b) The specimen of welded joint after tensile test.

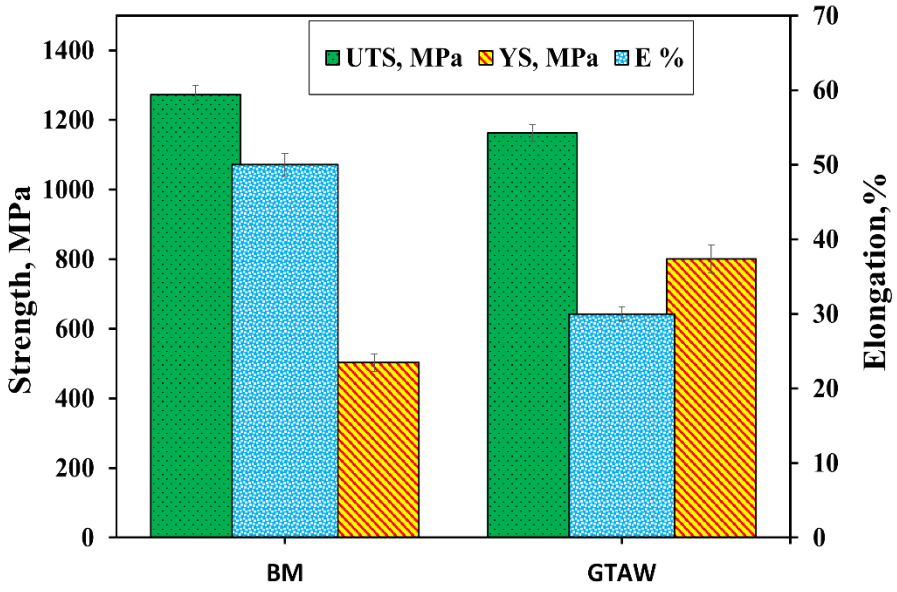

Fig. 9 Mechanical properties, ultimate tensile strength, yield strength, and elongation of 2507 SDSS BM and GTAWed samples.

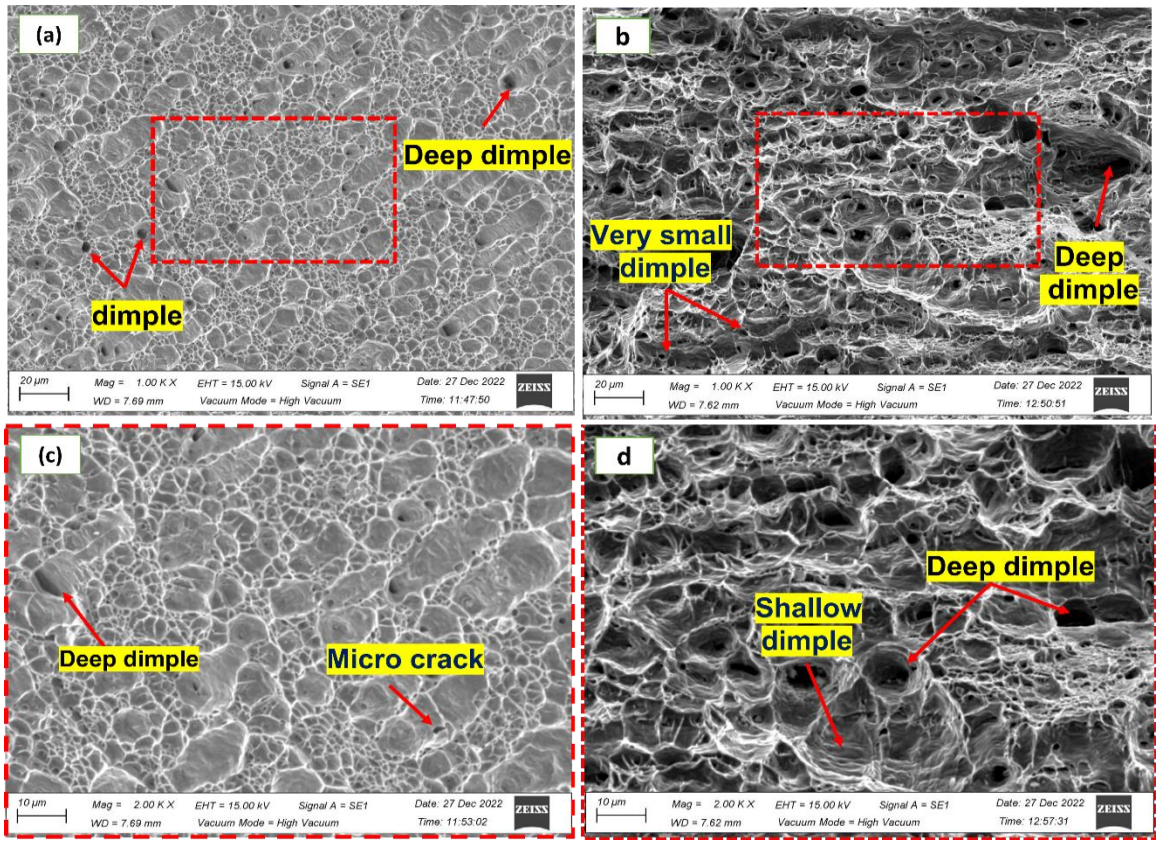

Fig. 10 SEM microphotographs of the fracture area of (a) BM, (b) the GTAWed sample, (c) a magnified image of the BM within the dashed rectangular area, and (d) a magnified image of the GTAWed sample within the dashed rectangular area.

Figure 10a shown SEM micrographs of the fracture area of the 2507 SDSS BM in the tensile test samples. The micrographs reveal elongated grains of both austenite (γ) and ferrite (α) phases aligned at a 45º degree angle, indicating the presence of ductile deformation in the BM sample as shown in figure 10c. Ductile fractures are characterized by extensive plastic deformation and the presence of elongated dimples, deep dimples in different sizes and shapes (elongated and rounded) on the fracture surface. On the other hand, Figure 10b displays clear evidence of microstructural changes resulting from GTAWed. it is disclosed in the form of Shallow dimples and micro-cracks These features indicate ductile fracture mode. During the tensile test, the original microstructure experiences high stress, leading to significant plastic deformation. This induces distortions in the form of shallow dimples, as presents in figure 10d.

CONCLUSIONS

The impact of various multi-pass gas tungsten arc welding parameters, including type of filler electrode, interpass temperature, and heat inputs on the microstructural characteristics and mechanical properties of 2507 SDSS welds was investigated and assessed. From the results obtained, the following conclusions can be drawn:

1- Attaining sound and flawless joints of 2507 super-duplex stainless steels is possible through multi-pass GTAW with the utilization of ER2594 filler material.

2- Significant hardness improvements were observed in the weld zone for the GTAWed joint reached up to 348 HV compared to the BM of 310 HV.

3- The welded joint achieved an ultimate tensile strength relatively close to the BM, but substantial improvements in yield strength were noted compared to the BM. Specifically, the yield strength of the welded joint increased by 59% compared to the BM.

4- Within the weld zone's microstructure, three distinct austenite forms were evident: Widmanstatten austenite (WA), intra-granular austenite (IGA), and grain boundary austenite (GBA), alongside the presence of ferrite.

5- The welding parameters influence the proportion of α and γ phases within the weld zone. In the GTAW-welded joint, the percentages of α and γ phases are 43% and 57%, respectively. These phase ratios are relatively close to natural balance ratios of α and γ found in the base metal, which are 50.6% and 49.4%, respectively. These findings support the utilization of multi-pass GTAW for welding 2507 SDSS, particularly when employing the recommended welding parameters as outlined in this study.

REFERENCES

1. Arun D., Devendranath Ramkumar K.,and Vimala R. ''Multi-Pass Arc Welding Techniques of 12 mm Thick Super-Duplex Stainless Steel.'', J. Mater. Process. Technol. 2019, 271, 126–143, doi:10.1016/j.jmatprotec.03.031, (2019).

2. Ahmed M.M.Z., Hajlaoui K., El-Sayed Seleman M.M., Elkady M.F., Ataya S., Latief F.H.,and Habba M.I.A. ''Microstructure and Mechanical Properties of Friction Stir Welded 2205 Duplex Stainless Steel Butt Joints.'', Materials (Basel), 14, 1–18, doi:10.3390/ma14216640, (2021).

3. Devendranath Ramkumar K., Mishra D., Thiruvengatam G., Sudharsan S.P.,

Mohan T.H., Saxena V., Rachit, P., and Arivazhagan N. ''Investigations on the Microstructure and Mechanical Properties of Multi-Pass PCGTA Welding of Super-Duplex Stainless Steel.'', Bull. Mater. Sci., 38, 837–846, doi:10.1007/s12034-015-0915-y, (2015).

4. Paulraj P.,and Garg R. ''Effect of Welding Parameters on Pitting Behavior of GTAW of DSS and Super DSS Weldments.'', Eng. Sci. Technol. an Int. J, 19, 1076–1083, doi:10.1016/j.jestch.2016.01.013, (2016).

5. Eghlimi A., Shamanian M., and Raeissi K. ''Effect of Current Type on Microstructure and Corrosion Resistance of Super Duplex Stainless Steel Claddings Produced by the Gas Tungsten Arc Welding Process.'', Surf. Coatings Technol. 2014, 244, 45–51, doi:10.1016/j.surfcoat.01.047, (2014).

6. Andersson J. ''Welding Metallurgy and Weldability of Superalloys.'', Metals (Basel)., 10, (2020).

7. Ramakrishnan P. ''Welding Metallurgy'',Vol. 4; ISBN 3175723993, (1972).

8. Beheshty M.A., Dehkordi E.H., Naghsh K.Z.,and Marnany M.R.B. ''Effects of Welding Cycles on Microstructural Characteristics and Mechanical Properties of SAF 2507 Super Duplex Stainless Steel.'', 2, 5–14, (2018).

9. Du D., Liu J., Li G., and Liu J. ''Effect of N2 Addition on Microstructure and Properties of Saf 2507duplex Stainless Steels Gtaw Welded Joint.'', Mater. Sci. Forum, 724, 127–130, doi:10.4028/www.scientific.net/MSF.724.127, (2012).

10. Devendranath Ramkumar K., Thiruvengatam G., Sudharsan S.P., Mishra D., Arivazhagan N., and Sridhar R.'' Characterization of Weld Strength and Impact Toughness in the Multi-Pass Welding of Super-Duplex Stainless Steel UNS 32750.'', Mater. Des., 60, 125–135, doi:10.1016/j.matdes.2014.03.031, (2014).

11. Zhu M., He F., Yuan Y.F., Yin S.M., Guo S.Y.,and Pan J. ''Effect of Aging Time on the Microstructure and Corrosion Behavior of 2507 Super Duplex Stainless Steel in Simulated Marine Environment.'', J. Mater. Eng. Perform., 30, 5652–5666, doi:10.1007/s11665-021-05812-2, (2021).

12. Yousefieh M., Shamanian M., and Saatchi A. ''Influence of Heat Input in Pulsed Current GTAW Process on Microstructure and Corrosion Resistance of Duplex Stainless Steel Welds.'', J. Iron Steel Res. Int, 18, 65–69, doi:10.1016/S1006-706X(12)60036-3, (2011).

13. Ahmed M.M.Z., Abdelazem K.A., El-Sayed Seleman M.M., Alzahrani B., Touileb K., Jouini N., El-Batanony I.G., and Abd El-Aziz H.M. ''Friction Stir Welding of 2205 Duplex Stainless Steel: Feasibility of Butt Joint Groove Filling in Comparison to Gas Tungsten Arc Welding.'', Materials (Basel), 14, 1–21, doi:10.3390/ma14164597, (2021).

14. Srirangan A.K.,and Paulraj S.'' Multi-Response Optimization of Process Parameters for TIG Welding of Incoloy 800HT by Taguchi Grey Relational Analysis. Eng. Sci. Technol. an Int. J, 19, 811–817, doi:10.1016/j.jestch.2015.10.003, (2016).

15. Yang Y., Yan B., Li J.,and Wang J. ''The Effect of Large Heat Input on the Microstructure and Corrosion Behaviour of Simulated Heat Affected Zone in 2205 Duplex Stainless Steel.'', Corros. Sci, 53, 3756–3763, doi:10.1016/j.corsci.2011.07.022, (2011).

16. Shin Y.T., Shin H.S., and Lee H.W. ''Effects of Heat Input on Pitting Corrosion in Super Duplex Stainless Steel Weld Metals.'', Met. Mater. Int, 18, 1037–1040,

doi:10.1007/s12540-012-6017-0, (2012).
17. Muthupandi V., Bala Srinivasan P., Seshadri S.K., and Sundaresan S. ''Effect of Weld Metal Chemistry and Heat Input on the Structure and Properties of Duplex Stainless Steel Welds.'', Mater. Sci. Eng. A, 358, 9–16, doi:10.1016/S0921-5093(03)00077-7, (2003).
18. Chen L., Tan H., Wang Z., Li J., and Jiang Y. ''Influence of Cooling Rate on Microstructure Evolution and Pitting Corrosion Resistance in the Simulated Heat-Affected Zone of 2304 Duplex Stainless Steels.'', Corros. Sci., 58, 168–174, doi:10.1016/j.corsci.2012.01.018, (2012).
19. Engineers P. ''The Eighteenth (2008) International.'', ISBN 9781880653708, (2008).
20. Welding Practice for the Sandvik Duplex Stainless Steels SAF 2304 , SAF 2205 Welding Practice for the Sandvik Duplex Stainless Steels SAF 2304 , SAF 2205 and SAF 2507 André de Albuquerque Vicente – M . Sc . Sandvik Materials Technology Do Brasil.
21. Tavares S.S.M., Pardal J.M., Lima L.D., Bastos I.N., Nascimento A.M.,and de Souza J.A. ''Characterization of Microstructure, Chemical Composition, Corrosion Resistance and Toughness of a Multipass Weld Joint of Superduplex Stainless Steel.'', UNS S32750. Mater. Charact. 2007, 58, 610–616, doi:10.1016/j.matchar.07.006, (2006).
22. Ferro P., Tiziani A., and Bonollo F. ''Influence of Induction and Furnace Postweld Heat Treatment on Corrosion Properties of SAF 2205 (UNS 31803). Weld.'', J. (Miami, Fla), 87, (2008).
23. Sun J., Li X., Sun Y., Jiang Y., and Li J. ''A Study on the Pitting Initiation of Duplex Stainless Steel (DSS 2205) Welded Joints Using SEM-EDS, SKPFM and Electrochemistry Methods.'', Int. J. Electrochem. Sci. 2018, 13, 11607–11619, doi:10.20964/12.54, (2018).
24. García-Rentería M.A., López-Morelos V.H., García-Hernández R., Dzib-Pérez L., García-Ochoa E.M., González-Sánchez J. '' Improvement of Localised Corrosion Resistance of AISI 2205 Duplex Stainless Steel Joints Made by Gas Metal Arc Welding under Electromagnetic Interaction of Low Intensity.'', Appl. Surf. Sci, 321, 252–260, doi:10.1016/j.apsusc.2014.10.024, (2014).
25. ASTM E8 ASTM E8/E8M Standard Test Methods for Tension Testing of Metallic Materials 1. Annu. B. ASTM Stand. 4, 1–27, doi:10.1520/E0008, (2010).
26. Gupta A., Kumar A., Baskaran T., Arya S.B., and Khatirkar R.K. ''Effect of Heat Input on Microstructure and Corrosion Behavior of Duplex Stainless Steel Shielded Metal Arc Welds. Trans.'', Indian Inst. Met, 71, 1595–1606, doi:10.1007/s12666-018-1294-z, (2018).
27. Wang L., Zhao P., Pan J., Tan L., and Zhu K. '' Investigation on Microstructure and Mechanical Properties of Double-Sided Synchronous TIP TIG Arc Butt Welded Duplex Stainless Steel.'', Int. J. Adv. Manuf. Technol, 112, 303–312, doi:10.1007/s00170-020-06375-7, (2021).
28. A Hosseini V., Hurtig K., Eyzop D., Östberg A., Janiak P., Karlsson L. ''Ferrite Content Measurement in Super Duplex Stainless Steel Welds.'', Weld. World, 63, 551–563, doi:10.1007/s40194-018-00681-1, (2019).
29. Nowacki J., Łukojć A. ''Structure and Properties of the Heat-Affected Zone of

Duplex Steels Welded Joints.'', J. Mater. Process. Technol, 164–165, 1074–1081, doi:10.1016/j.jmatprotec.2005.02.243, (2005).
30. Świerczyńska A., Łabanowski J., Fydrych D. '' The Effect of Welding Conditions on Mechanical Properties of Superduplex Stainless Steel Welded Joints.'', Adv. Mater. Sci., 14, 14–23, doi:10.2478/adms-2014-0002, (2014).
31. Xie X. fang, Li J., Jiang W., Dong Z., Tu S.T., Zhai X., Zhao X. '' Nonhomogeneous Microstructure Formation and Its Role on Tensile and Fatigue Performance of Duplex Stainless Steel 2205 Multi-Pass Weld Joints.'', Mater. Sci. Eng. A, 786, 139426, doi:10.1016/j.msea.2020.139426, (2020).